HHS Public Access

Author manuscript

J Magn Reson Imaging. Author manuscript; available in PMC 2015 April 30.

Published in final edited form as:

J Magn Reson Imaging. 2008 June ; 27(6): 1406–1411. doi:10.1002/jmri.21369.

Evaluation of Neovessels in Atherosclerotic Plaques of Rabbits Using an Albumin-Binding Intravascular Contrast Agent and MRI

Jean-Christophe Cornily, MD[1,2], **Fabien Hyafil, MD**[1,3], **Claudia Calcagno, MD**[1], **Karen C. Briley-Saebo, PhD**[1], **James Tunstead, PhD**[4], **Juan-Gilberto S. Aguinaldo, MD**[1], **Venkatesh Mani, PhD**[1], **Vito Lorusso, PhD**[5], **Friedrich M. Cavagna, PhD**[5], and **Zahi A. Fayad, PhD**[1,*]

[1]Imaging Science Laboratories, Mount Sinai School of Medicine, New York, New York.

[2]Department of Cardiology, Hôpital de la Cavale Blanche, CHU Brest, Brest, France.

[3]Department of Cardiology, Hôpital Bichat, Assistance Publique-Hopitaux de Paris, Paris, France.

[4]Department of Medicine and Michael A. Wiener Cardiovascular Institute, New York, New York.

[5]Bracco Imaging S.p.A., Milano, Italy.

Abstract

Purpose—To test whether B-22956/1, a novel intravascular contrast agent with a high affinity to serum albumin (Bracco Imaging SpA.), allowed quantifying neovessel and macrophage density in atherosclerotic plaques of rabbits using MRI.

Materials and Methods—A T1-weighted MRI of the aorta was acquired in 10 rabbits (7 atherosclerotic and 3 control rabbits) before and up to 2 h after intravenous injection of 100 μmol/kg of Gd-DTPA or 75 μmol/kg of B-22956/1. Plaque enhancement was measured at different time points. Immunohistochemistry was performed using anti-CD 31 antibodies and anti-RAM 11 antibodies to correlate to neovessel and macrophage density, respectively.

Results—MRI showed a significant plaque enhancement 2 h after B-22956/1 versus Gd-DTPA in the atherosclerotic group (39.75% versus 9.5%; $P < 0.0001$. Early atherosclerotic plaques (n = 146) enhancement positively correlates with neovessel density on corresponding histological sections (r = 0.42; $P < 0.01$). Enhancement of atherosclerotic plaques 2 h after injection of B-22956/1 correlated with macrophage density (r = 0.71; $P < 0.01$).

Conclusion—Enhancement of atherosclerotic plaques with MRI correlated with neovessel density at early time points after the injection of B-22956/1 and with macrophage density, at later time points. Hence, B-22956/1-enhanced MRI represents a promising imaging technique for the identification of “high-risk” plaques.

Keywords

atherosclerosis; magnetic resonance imaging; plaque; inflammation

*Address reprint requests to: Z.A.F., Mount Sinai School of Medicine, Imaging Science Laboratories, One Gustave L. Levy Place, Box 1234, New York, NY 10029. zahi.fayad@mssm.edu.

MRI is currently recognized as one of the best imaging techniques for the quantification of vascular plaque burden and assessment of atherosclerotic plaque composition (1–3). The composition of atherosclerotic plaques governs their vulnerability to disruption and, hence, their propensity to cause acute cardiovascular events.

Pathological neovascularization of the vessel wall plays a key role in atherosclerotic plaque development and progression (4,5). Increased neovascularization has been detected in ruptured human aortic plaques and is frequently associated with markers of plaque vulnerability such as intraplaque hemorrhage and thin-cap fibroatheromas (6,7).

Several different MRI techniques aspiring to assess plaque neovascularization have been described recently. Injection of $\alpha_v\beta_3$-integrin–targeted, paramagnetic nanoparticles provide specific detection of the neovasculature (8). Another approach is based on the evaluation of the early diffusion in atherosclerotic plaques of nonspecific extracellular MR contrast agents. Dynamic contrast-enhanced MRI (DCE-MRI) requires MR sequences with a fast acquisition of signal intensities in plaques and the development of models that estimate early diffusion of the extracellular contrast agent. Using this technique, the fractional blood volume represents a good estimation of the partial blood volume (ν_p) (9).

Gadolinium-based blood-pool contrast agents are currently developed to improve the accuracy of angiographies using MRI. According to their chemical structures, distribution of blood-pool contrast agents in the body is partially (albumin-binding contrast agents and rapid-clearance blood-pool contrast agents) or totally restricted to the plasma volume (slow-clearance blood-pool contrast agent). Gadocoletic acid trisodium salt (B-22956/1) is a novel blood-pool contrast agent that binds with a high affinity to serum albumin. B-22956/1 previously showed its interest in coronary MR angiography in animals (10) and humans (healthy volunteers [11] or patients with known or suspected coronary artery disease [12]). As acute arterial syndromes (unstable angina, acute myocardial infarction, transient ischemic attack, stroke) are caused, in approximately twothirds of patients, by the endothelial disruption of “high-risk atherosclerotic plaques” (13,14), nonstenotic plaque detection and plaque characterization have become a major goal for modern science. Thus, a contrast agent that could be used in both angiography and plaque characterization would be highly valuable. B-22956/1 has been tested in preliminary clinical studies as a blood-pool contrast agent for MRI. We tested whether, at the dose used for angiographies, B-22956/1 could (i) improve atherosclerotic plaque detection and (ii) help to detect atherosclerotic plaques prone to rupture. We hypothesized that the enhancement of atherosclerotic plaques at early time point with a preponderant intravascular location of B-22956/1, would correlate with neovessel density. At later imaging time points, B-22956/1 could diffuse through leaky neovessels and correlate to macrophage density.

MATERIALS AND METHODS

Animal Protocol

Ten male New Zealand White (NZW) rabbits (mean age, 4 months; mean weight = 3.4 ± 0.2 kg; Covance, Princeton, NJ) were included in this study. Aortic atherosclerosis plaques were induced in 7 rabbits by a combination of 4 months of high cholesterol diet (4.7% coconut oil

and 0.3% cholesterol-enriched diet; Research Diet Inc., New Brunswick, NJ) and a double balloon denudation injury of the aorta (2 weeks and 6 weeks after starting the high-cholesterol diet). Injury was performed from the aortic arch to the iliac bifurcation with a 4F Fogarty embolectomy catheter introduced through the femoral artery. All procedures were performed under general anesthesia by an intramuscular injection of ketamine (20 mg/kg; Fort Dodge Animal Health, Overland Park, KS) and xylazine (10 mg/kg; Bayer Corp., Shawnee Mission, KS). Three noninjured rabbits, fed a normal chow diet, were used as controls. All experiments were approved by the institutional Animal Care and Use Committee.

Contrast Agent

B-22956/1 is a novel, low molecular-weight (molecular mass = 1059 Dalton), gadolinium-based, MR blood-pool agent developed by Bracco Imaging SpA (Milan, Italy). Its international nonproprietary name is gadocoletic acid trisodium salt. Its apparent relaxivity as determined by measuring the relaxation rate of a 0.6 mM solution of the chelate in Seronorm® at 0.5 Tesla (T) is 27 $mM^{-1}s^{-1}$. In humans, blood T1 values at 1.5 T of 35 and 55 ms have been found, respectively, at 5 and 30 min after administration of 0.1 mmol/kg of B-22956/1. Its r1 = 27 mM^{-1} s^{-1} at 1.5 T in 39°C human serum is 27 mM^{-1} s^{-1} at 1.5 T. Protein binding, determined as bound fraction for 0.5 mM solutions of the Gd-complex in 0.6 mM Krebs–Ringer solutions of human and pig serum albumin, was 94% and 90%, respectively (15). A high rabbit-albumin binding level has also been measured > 90% (15).

MRI Protocol

Rabbits were anesthetized with an intramuscular injection (ketamine: 20 mg/kg, xylazine: 10 mg/kg and acepromazine [0.05 mL/kg; Fort Dodge Animal Health, Overland Park, KS]: 0.5 mg/kg) and imaged supine in a 1.5 T MRI system equipped with a 30 mT/m gradient system (Siemens Medical Solutions, Erlangen, Germany) using a conventional knee coil. Sequential transverse images of the abdominal aorta, from the renal arteries to the iliac bifurcation, were obtained with a T1-weighted, two-dimensional (2D), high-resolution black blood fast spin-echo sequence using the following parameters: repetition time = 800 ms; echo time = 5.6 ms; echo train length = 7; received bandwidth = 488 Hz per pixel; slice thickness = 3 mm; acquisition matrix = 256 × 256; field of view = 100 mm × 100 mm; number of signal averages = 4; number of slices = 22; sequence duration = 7 min 56 s; in-plane spatial resolution = 0.45 × 0.4 mm.

Inferior and superior radiofrequency saturation pulses were added to null the signal from flowing blood in the inferior vena cava and aorta and spectral fat suppression, to null the signal from the periadventitial fat.

T1-weighted imaging was performed before and continuously up to 2 h after injection for both contrast agents: Gd-DTPA (100 μmol/kg) intravenous injection (IV) on day 1 and B-22956/1 (75 μmol/kg) IV, 1 week later.

Image and Data Analysis

All images were analyzed on a Leonardo workstation (Siemens Medical Solutions). For each time point (before injection, 8 min, 16 min, 30 min, 60 min, 90 min, 120 min), the 22 axial images were analyzed along the abdominal aorta. Contours were manually drawn around the aorta lumen and on the outer wall boundary, including the adventitia. Signal intensities (SI) in arterial wall regions of interest (ROI) were measured by an experienced observer. An ROI containing no motion artifact was placed outside the animal to measure the standard deviation of the noise signal (SDN) and another was placed in a homogenous region of the muscle (psoas muscle) to allow for calculation of the plaque enhancement (PE). Signal to noise ratio (SNR) was defined as: SNR = SI/SDN at the same time point; signal increase (SIn) = SNR_{post}/SNR_{pre};; plaque enhancement (PE) = $(SI_{plaque\ post}/SI_{muscle\ post})/(SI_{plaque\ pre}/SI_{muscle\ pre}) \times 100 - 100$.

Histological Analysis

After the second MRI, rabbits were killed by an intravenous injection of 120 mg/kg of sodium pentobarbital (Sleepaway; Fort Dodge Animal Health). A bolus of heparin was injected before killing to prevent clot formation. Aortas were excised, fixed for 24 h in 4% paraformaldehyde, and embedded in paraffin. We ensured concordance between the position of the MR slices and the corresponding histological slices using anatomical reference such as iliac bifurcation, right renal artery, and diaphragmatic crossing. Five-micrometer-thick slices were sectioned in the same direction as MRI slices and stained with hematoxylin–eosin. Additional sections from each location were then stained using a CD-31 antibody which binds to endothelial cells and a RAM-11 antibody which binds to macrophages. A magnification factor of 40 was used for microvessel analysis and 2 for macrophage analysis. Microvessel density was calculated by measuring the total number of microvessels in atherosclerotic plaques and dividing by total plaque area. A vessel wall microvessel density was also calculated taking into account the global wall area (plaque area + adventitia). Macrophage density was calculated using morphometric analysis software (Image-Pro Plus; Media Cybernetics, Silver Spring, MD). Macrophage content was measured by quantifying the brown area on sections stained with a RAM-11 antibody. The total macrophage area was normalized by dividing the total plaque area and was expressed as percentages.

Statistical Analysis

Statistical analysis was conducted with SPSS software (SPSS Inc., Chicago, IL). All probabilities were two-sided and expressed as mean ± standard deviation. Plaque enhancements were compared using a Student's *t*-test for paired samples. The relationship between the histological variables (plaque neovessel density, arterial wall neovessel density, and plaque macrophage density) and the MRI variable (signal increase, plaque enhancement) were evaluated by computing Pearson's correlation coefficient r. Values of $P < 0.05$ were considered as significant.

RESULTS

We detected a significant higher plaque enhancement 2 h after B22956/1 (Figs. 1, 2) versus Gd-DTPA in the atherosclerotic group with T1-weighted MR sequences (39.75 ± 0.04% versus 9.5 ± 0.06%, respectively; $P < 0.0001$).

We measured a mean plaque enhancement of 13.9%, 24.1%, 31.2%, 38.8%, and 39.75% at 16, 30, 60, 90, and 120 min after the injection of B-22956/1, respectively. Plaque enhancement significantly increased up to 90 min ($P < 0.001$ between 0 and 15 min, $P < 0.001$ between 16 and 30 min, $P < 0.001$ between 30 and 60 min, and $P < 0.001$ between 60 and 90 min), and then reached a plateau between 90 and 120 min (P = nonsignificant [ns]). In contrast, we detected a plaque enhancement of only 18.3%, 28.1%, 20.6%, 14.3%, 11.0%, and 9.5% at 8, 16, 30, 60, 90, and 120 min after the injection of Gd-DTPA, respectively.

In the atherosclerotic group, the higher plaque enhancement was measured at 39.75% 2 h after injection of B22956/1 as compared to only 28.3% 16 min after injection of Gd-DTPA. ($P < 0.001$).There was no difference in plaque enhancement between B22956/1 and Gd-DTPA in control rabbits (15 ± 0.01% versus 15 ± 0.01%; P = ns).

Twenty-two segments of aortas were analyzed per atherosclerotic rabbit; thus, the number of sections should have been 154. Eight aorta levels were useless for histological (bad quality of the sections that made the aorta seem not circular [paraffin-embedding mistake]) or image (bad quality of the corresponding MR images) analysis; bad quality slices were excluded, and 146 blocks were finally compared with the corresponding 146 MR axial slices.

In atherosclerotic rabbits, we found a strong correlation between plaque enhancement (n = 146) at early time points (8 min after injection of B-22956/1) with plaque neovessel density (r = 0.42; $P < 0.01$). We calculated correlations (Figs. 3–5) between signal increase and macrophage density at different time points: r = 0.15 at t = 8 min (P = ns); r = 0.21 at t = 16 min (P = ns); r = 0.27 at t = 30 min (P = ns); r = 0.34 at t = 60 min ($P < 0.05$); r = 0.57 at t = 90 min ($P < 0.01$); r = 0.71 at t = 2 h ($P < 0.01$). We found no correlation between neovessel and macrophage densities (r = 0.12, P = ns).

DISCUSSION

We demonstrate in this study that B-22956/1, a new blood-pool contrast agent, provided a strong enhancement of atherosclerotic plaques of rabbits with MRI as compared to Gd-DTPA. In addition, we demonstrated that the enhancement of atherosclerotic plaques at early time points after the injection of B-22956/1 correlated with neovessel density and plaque enhancement at later time points, with macrophage density measured on corresponding arterial sections with immunohistology. Hence, B-22956/1-enhanced MIRI could represent an interesting imaging technique to improve identification and characterization of atherosclerotic plaques using MRI.

In previous studies, Gadofluorine (Schering AG) was shown to improve atherosclerotic plaque detection. However, Gadofluorine has a much higher relaxivity (R1) than B-22956/1. Hence, the discrimination between atherosclerotic plaques and lumen is hampered by a

persistent short T1 in blood. Even though dedicated MR acquisitions have been developed to null the luminal signal, the best time point for atherosclerotic plaque detection was estimated only at 24 h after injection (16).

Using an extracellular contrast agent such as Gd-DTPA and kinetic modeling of dynamic contrast-enhanced MRI, Kerwin et al (9) could calculate fractional blood volume that correlated with neovessel density in atherosclerotic plaques. However, this technique has two major drawbacks: First, conventional gadolinium-based contrast agents are characterized by rapid distribution into the extracellular space and a relatively rapid clearance by the kidneys. Therefore, the common approach is to use a two compartment model of contrast agent exchange that needs to take into account the early diffusion of contrast agent from the vascular system into the extravascular extracellular space. Second, this technique allows for the imaging of several slices but only one location can be selected for image analysis. In contrast, the prolonged intravascular phase of B-22956/1 could offer us to study different arterial territories (carotid, coronary, and peripheral arteries) at the same time using the new whole-body MRI systems.

Several intravascular contrast agents (e.g., dendritic contrast agents, MS 325 [EPIX Medical, Cambridge, MA] or [CMD]-A2-Gd-DOTA [Guerbet Laboratories, Aulnay sous bois, France]) tried to assess microvascularization of tumors with more or less success (17–19). MS 325 provided good results mainly for angiography (20,21), but also to assess blood volume in experimental tumors. Its good safety profile allowed it to be marketed in Europe.

Recently, B-22956/1 was successfully used to assess the effect of antiangiogenic treatment in a rat model of breast cancer (22). However, to our knowledge, this is the first time that a blood-pool contrast agent has demonstrated its ability to assess plaque microvasculature.

Macrophages could be detected with MRI using USPIO in atherosclerotic plaques of hyperlipidemic rabbits (23) and human carotid arteries (24). After phagocytosis by macrophages, USPIO can be detected through susceptibility effects using T2*-weighted MR sequences. However, the best imaging time point after the injection of USPIO was estimated at 36 h, which strongly limited its clinical use (25). In contrast, we demonstrated in the study that B-22956/1 could provide a reliable estimation of macrophage density in atherosclerotic plaque as soon as 90 min after the injection of the contrast agent, rendering more suitable for evaluation of atherosclerotic plaques in patients.

LIMITATIONS

In this study, we chose to compare both contrast agents at a clinical dose, which had been demonstrated effective and safe in humans. However, the higher relaxivity of B-22956 (r1 = 27 at 20 MHz, dose 75 μmol/kg) as compared to Gd-DTPA (r1 = 3.6 at 20 MHz, dose: 100 μmol/kg) could partially explain the higher enhancement detected in atherosclerotic plaques. Although matching MR imaging and histology was a priority in our work, the mandatory mismatch in slice-thickness (5 μm for histology and 3 mm for MRI) induces a certain level of inaccuracy in the results.

In conclusion, B-22956/1-enhanced MRI increases atherosclerotic plaque signal compared with Gd-DTPA. During the early phase after injection, the properties of B-22956/1 allow an estimation of plaque neovessel density. Two hours after injection, B-22956/1, probably linked to albumin, diffuses from the neovessels into the plaque with a signal increase that correlates to the macrophage density of the plaque.

ACKNOWLEDGMENTS

J.C.C. and F.H. were funded by the Federation Française de Cardiologie and Z.A.F. was funded by the NIH/NHLBI.

Contract grant sponsor: the Federation Française de Cardiologie; Contract grant sponsor: NIH/NHLBI; Contract grant number: R01 HL71021; Contract grant number: R01 HL78667.

REFERENCES

1. Yuan C, Lin E, Millard J, Hwang JN. Closed contour edge detection of blood vessel lumen and outer wall boundaries in black-blood MR images. Magn Reson Imaging. 1999; 17:257–266. [PubMed: 10215481]
2. Fayad ZA, Fuster V, Fallon JT, et al. Noninvasive in vivo human coronary artery lumen and wall imaging using black-blood magnetic resonance imaging. Circulation. 2000; 102:506–510. [PubMed: 10920061]
3. Choudhury RP, Fuster V, Badimon JJ, Fisher EA, Fayad ZA. MRI and characterization of atherosclerotic plaque: emerging applications and molecular imaging. Arterioscler Thromb Vasc Biol. 2002; 22:1065–1074. [PubMed: 12117718]
4. Jeziorska M, Woolley DE. Neovascularization in early atherosclerotic lesions of human carotid arteries: its potential contribution to plaque development. Hum Pathol. 1999; 30:919–925. [PubMed: 10452504]
5. Barger AC, Beeuwkes R III, Lainey LL, Silverman KJ. Hypothesis: vasa vasorum and neovascularization of human coronary arteries. A possible role in the pathophysiology of atherosclerosis. N Engl J Med. 1984; 310:175–177. [PubMed: 6197652]
6. Moreno PR, Purushothaman KR, Fuster V, et al. Plaque neovascularization is increased in ruptured atherosclerotic lesions of human aorta: implications for plaque vulnerability. Circulation. 2004; 110:2032–2038. [PubMed: 15451780]
7. Virmani R, Kolodgie FD, Burke AP, et al. Atherosclerotic plaque progression and vulnerability to rupture: angiogenesis as a source of intraplaque hemorrhage. Arterioscler Thromb Vasc Biol. 2005; 25:2054–2061. [PubMed: 16037567]
8. Winter PM, Morawski AM, Caruthers SD, et al. Molecular imaging of angiogenesis in early-stage atherosclerosis with alpha(v)beta3- integrin-targeted nanoparticles. Circulation. 2003; 108:2270–2274. [PubMed: 14557370]
9. Kerwin W, Hooker A, Spilker M, et al. Quantitative magnetic resonance imaging analysis of neovasculature volume in carotid atherosclerotic plaque. Circulation. 2003; 107:851–856. [PubMed: 12591755]
10. Zheng J, Li D, Maggioni F, et al. Single-session magnetic resonance coronary angiography and myocardial perfusion imaging using the new blood pool compound B-22956 (gadocoletic acid): initial experience in a porcine model of coronary artery disease. Invest Radiol. 2005; 40:604–613. [PubMed: 16118554]
11. Paetsch I, Huber ME, Bornstedt A, et al. Improved three-dimensional free-breathing coronary magnetic resonance angiography using gadocoletic acid (B-22956) for intravascular contrast enhancement. J Magn Reson Imaging. 2004; 20:288–293. [PubMed: 15269955]
12. Paetsch I, Jahnke C, Barkhausen J, et al. Detection of coronary stenoses with contrast enhanced, three-dimensional free breathing coronary MR angiography using the gadolinium-based intravascular contrast agent gadocoletic acid (B-22956). J Cardiovasc Magn Reson. 2006; 8:509–516. [PubMed: 16755840]

13. Naghavi M, Libby P, Falk E, et al. From vulnerable plaque to vulnerable patient: a call for new definitions and risk assessment strategies: Part I. Circulation. 2003; 108:1664–1672. [PubMed: 14530185]
14. Virmani R, Burke AP, Farb A, Kolodgie FD. Pathology of the vulnerable plaque. J Am Coll Cardiol. 2006; 47:C13–C18. [PubMed: 16631505]
15. de Haen C, Anelli PL, Lorusso V, et al. Gadocoletic Acid trisodium salt (b22956/1): a new blood pool magnetic resonance contrast agent with application in coronary angiography. Invest Radiol. 2006; 41:279–291. [PubMed: 16481911]
16. Sirol M, Itskovich VV, Mani V, et al. Lipid-rich atherosclerotic plaques detected by gadofluorine-enhanced in vivo magnetic resonance imaging. Circulation. 2004; 109:2890–2896. [PubMed: 15184290]
17. Krause MH, Kwong KK, Xiong J, Gragoudas ES, Young LH. MRI of blood volume with MS 325 in experimental choroidal melanoma. Magn Reson Imaging. 2003; 21:725–732. [PubMed: 14559336]
18. Preda A, Novikov V, Moglich M, et al. Magnetic resonance characterization of tumor microvessels in experimental breast tumors using a slow clearance blood pool contrast agent (carboxymethyldextran- A2-Gd-DOTA) with histopathological correlation. Eur Radiol. 2005; 15:2268–2275. [PubMed: 16012822]
19. de Lussanet QG, Langereis S, Beets-Tan RG, et al. Dynamic contrast- enhanced MR imaging kinetic parameters and molecular weight of dendritic contrast agents in tumor angiogenesis in mice. Radiology. 2005; 235:65–72. [PubMed: 15731376]
20. Corot C, Violas X, Robert P, Gagneur G, Port M. Comparison of different types of blood pool agents (P792, MS325, USPIO) in a rabbit MR angiography-like protocol. Invest Radiol. 2003; 38:311–319. [PubMed: 12908698]
21. Port M, Corot C, Violas X, Robert P, Raynal I, Gagneur G. How to compare the efficiency of albumin-bound and nonalbumin-bound contrast agents in vivo: the concept of dynamic relaxivity. Invest Radiol. 2005; 40:565–573. [PubMed: 16118549]
22. Preda A, Novikov V, Moglich M, et al. MRI monitoring of Avastin antiangiogenesis therapy using B22956/1, a new blood pool contrast agent, in an experimental model of human cancer. J Magn Reson Imaging. 2004; 20:865–873. [PubMed: 15503324]
23. Hyafil F, Laissy JP, Mazighi M, et al. Ferumoxtran-10-enhanced MRI of the hypercholesterolemic rabbit aorta relationship between signal loss and macrophage infiltration. Arterioscler Thromb Vasc Biol. 2006; 26:176–181. [PubMed: 16269663]
24. Kooi ME, Cappendijk VC, Cleutjens KB, et al. Accumulation of ultrasmall superparamagnetic particles of iron oxide in human atherosclerotic plaques can be detected by in vivo magnetic resonance imaging. Circulation. 2003; 107:2453–2458. [PubMed: 12719280]
25. Ruehm SG, Corot C, Vogt P, Kolb S, Debatin JF. Magnetic resonance imaging of atherosclerotic plaque with ultrasmall superparamagnetic particles of iron oxide in hyperlipidemic rabbits. Circulation. 2001; 103:415–422. [PubMed: 11157694]

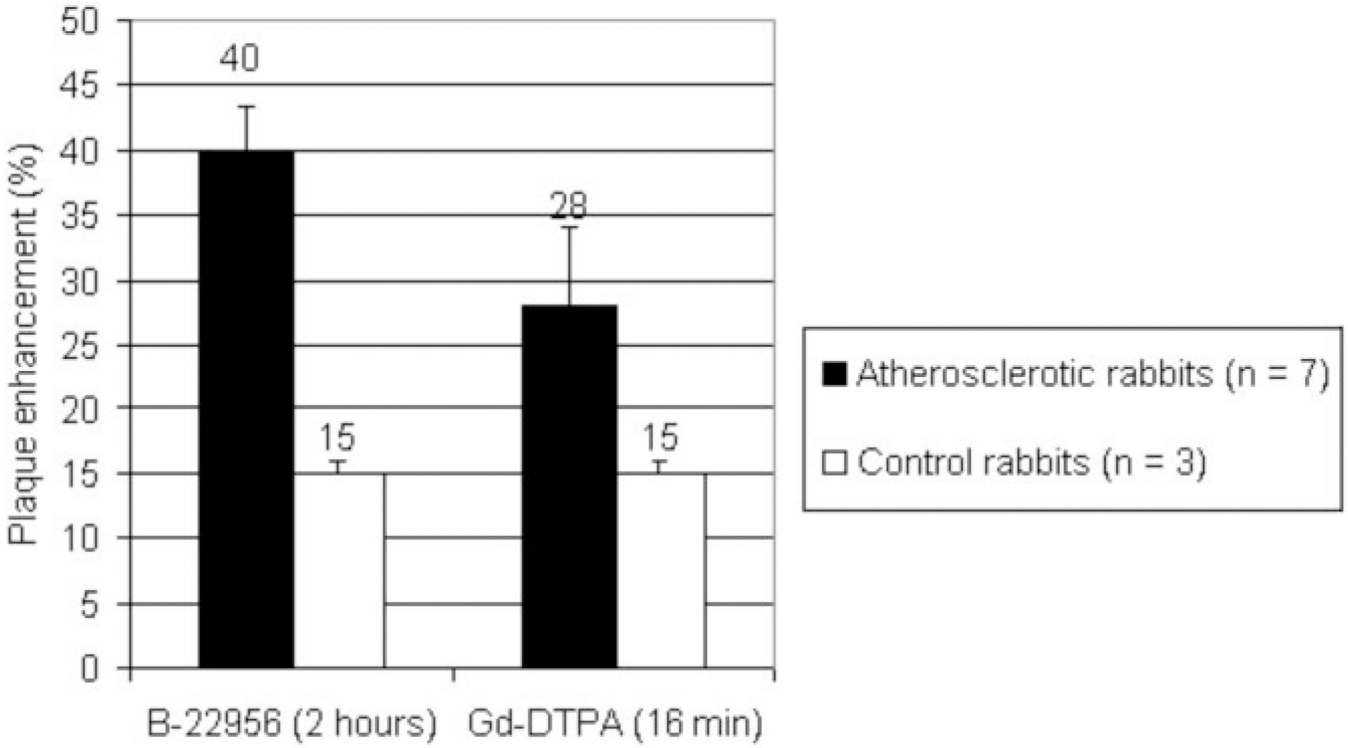

Figure 1.

Maximum plaque enhancement, 2 h after injection of B-22956/1 (75 μmol/kg) IV or 16 min after Gd-DTPA (100 μmol/kg) IV. We detected a significant stronger enhancement observed in atherosclerotic plaques after injection of B-22956 than after the injection of Gd-DTPA. No difference was found between the two compounds in control rabbits.

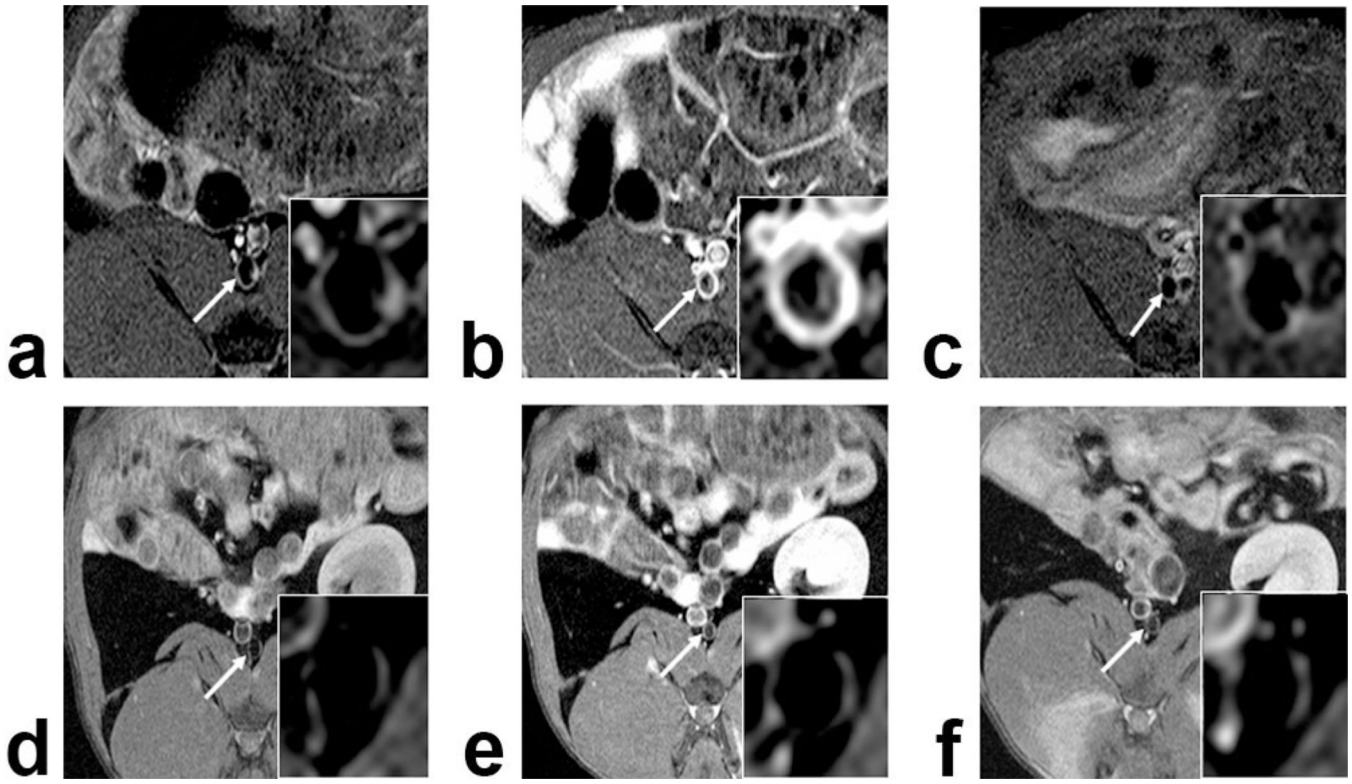

Figure 2.

Axial T1-Weighted MR images of atherosclerotic (**A–C**) and control (**D–F**) rabbit abdominal aortas: Precontrast imaging (A,D) and 2 h after B-22956/1 (B,E) or Gd-DTPA (C,F). We detected a strong enhancement of the atherosclerotic plaque 2 h after B-22956/1 injection, whereas no significant enhancement could be detected, neither after the injection of Gd-DTPA in atherosclerotic rabbits nor in the aortic of control rabbits after the injection of B-22956/1 and Gd-DTPA.

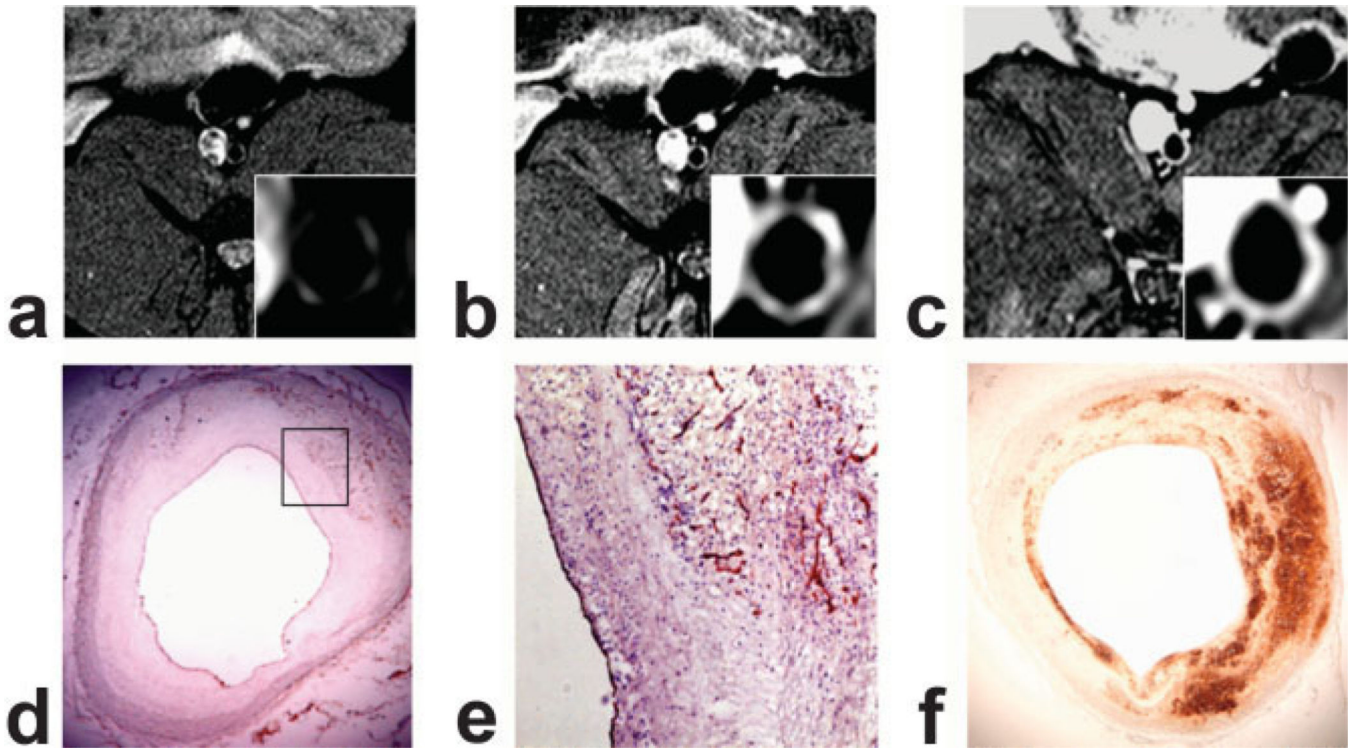

Figure 3.

Axial T1-weighted MR images of atherosclerotic rabbit abdominal aortas at three different time points: before injection of B-22956/1 (**A**), 8 min after injection (**B**), and 2 h after injection (C). Histological identification of neovessel (CD-31 immunostaining [**D,E**]) and macrophages (RAM-11 immunostaining [**F**]). B: Note the strong signal with a T1-weighted sequence at an early time point after the injection of B-22956/1 corresponding to a neovessel-rich area on the corresponding histological section (E). At later time points, we detected a diffuse enhancement of the same atherosclerotic plaque corresponding to a strong macrophage infiltration on corresponding cross-section of the atherosclerotic plaque (F).

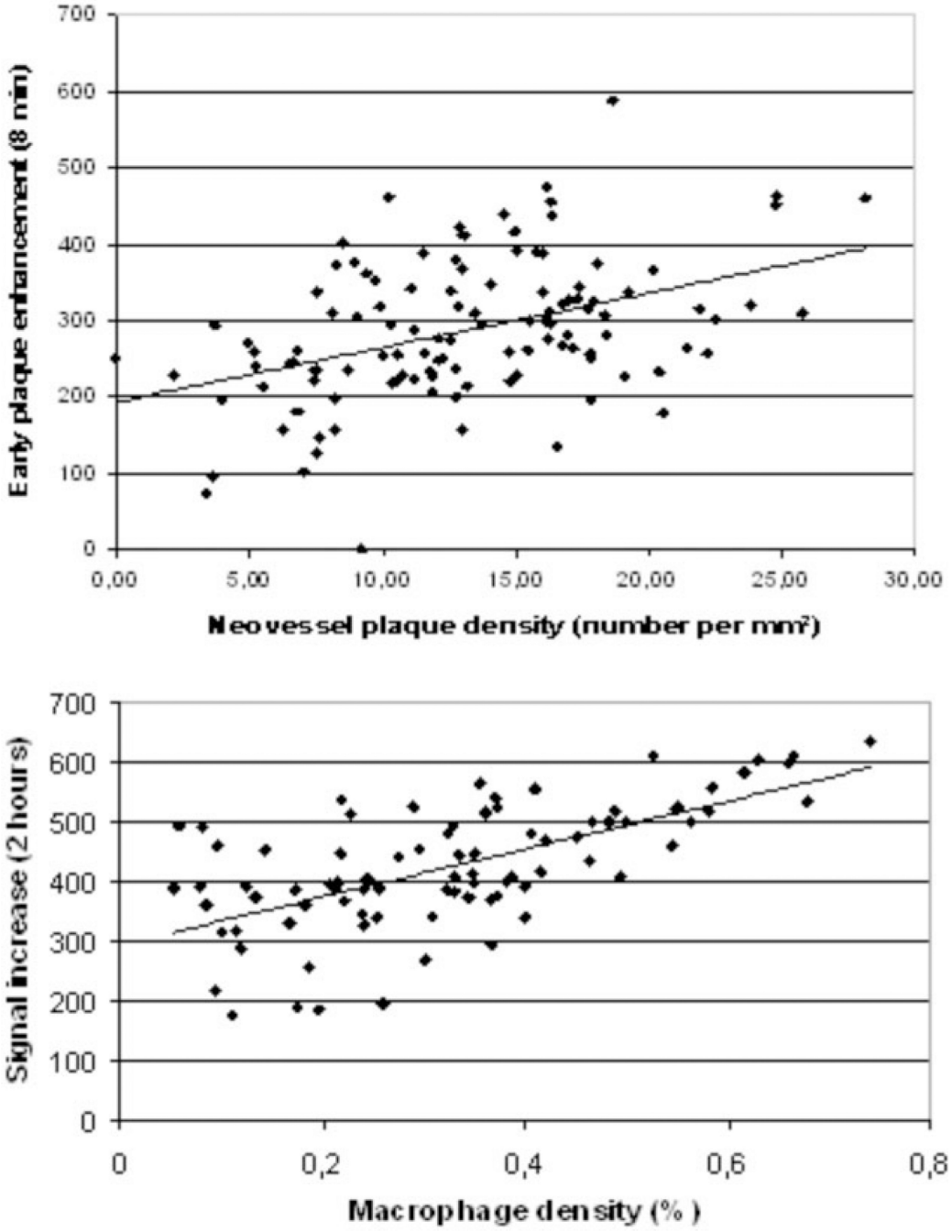

Figure 4.

A: Comparison of plaque enhancement by MRI and wall neovessel density by histology (number per mm^2). Measurement time point: 8 min. r = 0.42; $P < 0.01$. **B**: Comparison of signal increase 2 h after injection of B-22956/1 and macrophage density (in percent). Measurement time point: 120 min. r = 0.71, ($P < 0.01$). All regression lines are automatically drawn.

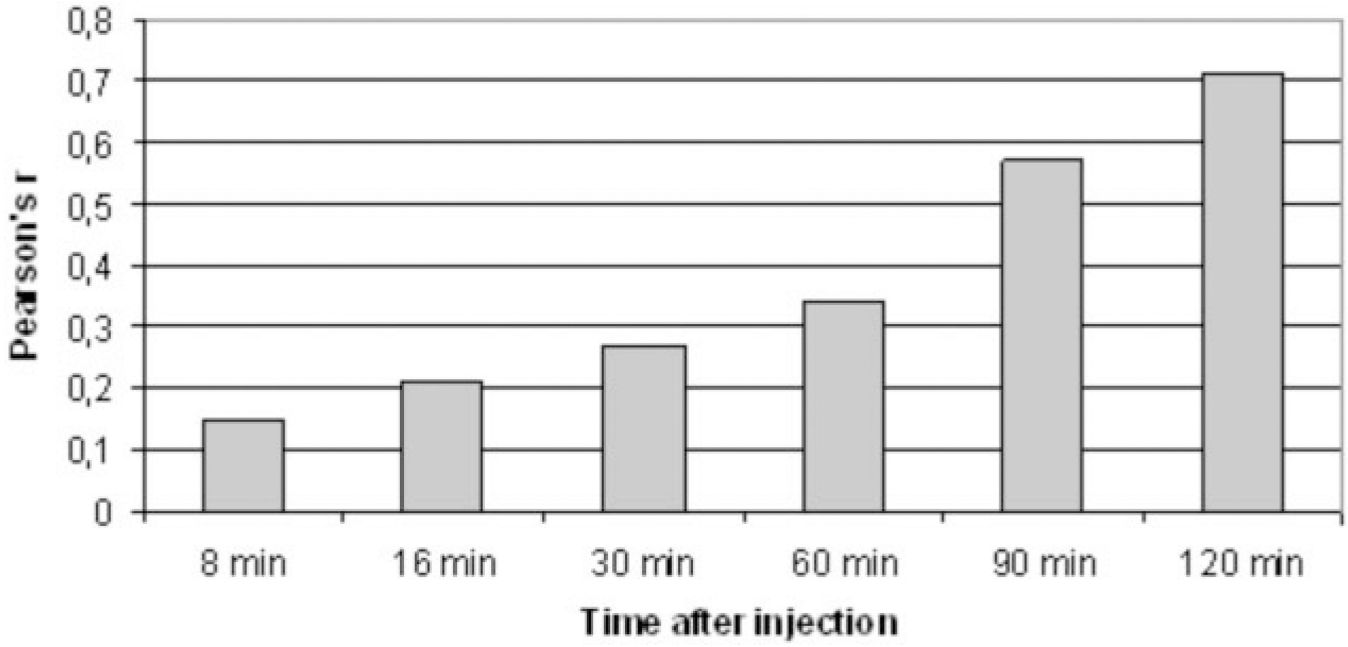

Figure 5.

Correlation between signal increase in atherosclerotic plaques of rabbits and macrophage density at different time points after the injection of B-22956/1. Correlation between plaque enhancement with MRI and macrophage density on corresponding sections is increasing with time delay after the injection of B-22956/1.